

Generative chemical transformer: attention makes neural machine learn molecular geometric structures via text

Hyunseung Kim[†], Jonggeol Na^{‡,*}, Won Bo Lee^{†,*}

[†]School of Chemical and Biological Engineering, Seoul National University, Gwanak-ro 1, Gwanak-gu, Seoul 08826, Republic of Korea

[‡]Division of Chemical Engineering and Materials Science, Ewha Womans University, Seoul 03760, Republic of Korea

Correspondence and requests for materials should be addressed to

J.N. (email: jgna@ewha.ac.kr) or W.B.L. (email: wblee@snu.ac.kr).

Abstracts

Chemical formula is an artificial language that expresses molecules as text. Neural machines that have learned chemical language can be used as a tool for inverse molecular design. Here, we propose a neural machine that creates molecules that meet some desired conditions based on a deep understanding of chemical language (generative chemical Transformer, GCT). Attention-mechanism in GCT allows a deeper understanding of molecular structures, beyond the limitations of chemical language itself that cause semantic discontinuity, by paying attention to characters sparsely. We investigate the significance of language models to inverse molecular design problems by quantitatively evaluating the quality of generated molecules. GCT generates highly realistic chemical strings that satisfy both a chemical rule and grammars of a language. Molecules parsed from generated strings simultaneously satisfy the multiple target properties and are various for a single condition set. GCT generates de novo molecules, and this is done in a short time that human experts cannot. These advances will contribute to improving the quality of human life by accelerating the process of desired material discovery.

Material discovery is a research field that searches for new materials that fit some specific purposes. Since the chemical space is vast, only organic molecules less than 500 daltons exceed 10^{60} ¹, searching molecular structures that simultaneously satisfy the multiple desired conditions requires a high level of expert knowledge and consumes a lot of time and cost. For this reason, inferring the desired molecules using artificial intelligence with transcendental learning capabilities can help to accelerate the process of material discovery.

In recent years, attempts have been made to utilize neural nets in chemistry fields where the relationship between molecular structure and physical properties is complex. Molecules are made up of atoms and bonds connecting themselves, so their nature is close to a graph. However, in the past when printing was not developed—it was difficult to use images of molecules, and for this reason—techniques for expressing molecules in the form of strings have been studied²⁻⁶. A simple example is to write aspirin as $C_9H_8O_4$, a chemical formula. Simplified molecular-input line-entry system (SMILES)⁴⁻⁶—developed in the 1980s—is the most popular artificial language used to express molecular structure in detail. Like natural language, SMILES strings are arranged in order according to grammar and context.

Several approaches have demonstrated that natural language processing (NLP) models are applicable to inverse molecular design problems by generating molecules expressed in chemical language via a language model itself to select a character that follows the currently generated string⁷⁻⁹, or a language model combined with variational autoencoder (VAE)¹⁰ to compress molecular information into latent space and re-sample the latent code to create various strings^{11,12}, or a language model combined with a generative adversarial network (GAN)¹³ to create strings from noise¹⁴, or a language model combined with reinforcement learning to reward a natural character that follows the currently generated string¹⁵. However, there is not much analysis on why language model-based molecular generators work well.

An important point in material discovery is the creation of molecular structures that meet desired multiple target conditions. To this end, by applying additional optimization or navigation to the process of generating molecules or to the latent space obtained from the generative model, the desired molecule can be generated in 2-step: Bayesian optimization^{11,16}, particle swarm optimization (PSO)¹⁷, genetic optimization (GA)¹⁸⁻²⁰, Monte Carlo tree search (MCTS)²¹⁻²³. Another method is to use conditional models, which create molecules with given target conditions in 1-step. The latter can shorten the time consumed to discover the desired molecules and directly control the molecules to be generated. For this reason, attempts have been made to directly input conditions to a recurrent neural network (cRNNs)²⁴. Unlike generative models, since recurrent neural network (RNN) is a model based on one-to-one matching, there is a limitation in using it as a tool to infer the various molecular candidates with a single condition set; here, the generative models refer to models that can output various results by decoding latent codes sampled from the distribution of latent variables (latent space).

Here, we propose generative chemical Transformer (GCT) that embeds Transformer²⁵—state-of-the-art architecture that became a breakthrough of NLP problems by using attention-mechanism²⁶—into a conditional variational generative model; to be precise, we adopt pre-layer normalization (pre-LN) Transformer²⁷ as a base language model of GCT, not the original Transformer which uses post-LN (the reason why we designed GCT like this is stated in **Methods**). From the point of view of data recognition and processing, GCT is close to a conditional variational generator that embodies the language recognition ability of attention in Transformer. To use GCT as a tool of material discovery, we intend to take advantage of both the high-performance language model and the conditional generative model. We analyze GCT by quantitatively evaluating the generated molecules and investigate the significance of language models to the inverse molecular design problems. We show that a deep understanding of molecular geometric structure learned from chemical language by paying attention to each character in chemical strings sparsely helps to generate chemical strings satisfying the chemical valance rule and syntax of the chemical language (grammar understanding).

And the strings are parsed into highly realistic molecules (contextual understanding). Also, we demonstrate that the conditional variational generator, which is the skeleton of GCT, helps to generate molecules that satisfy multiple preconditions simultaneously (conditional generator) and are various for a single precondition set (variational generator). Besides, the autoencoder, a substructure of GCT, makes the molecular size controllable.

Results and Discussion

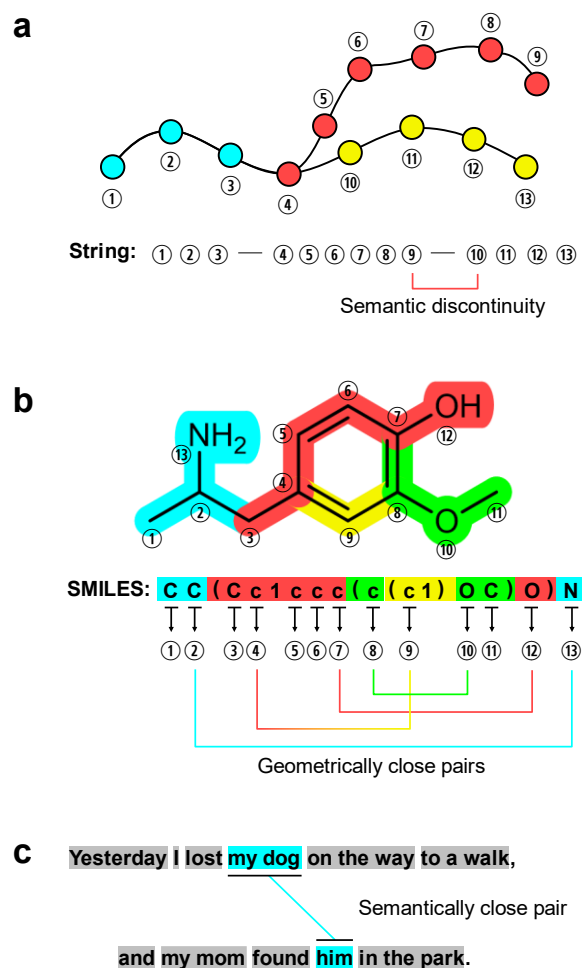


Fig. 1 Structural limitation of language forms. **a**, An example of a non-Hamiltonian graph. A Hamiltonian graph is a graph in that has a path that passes through all the points in the graph only once, and a non-Hamiltonian graph is not. **b**, An example of a non-Hamiltonian molecular graph and its SMILES string: 4-(2-Aminopropyl)-2-methoxyphenol. Each atom is labeled with a circled number. Different colors refer to different branches. **c**, In natural language, words that are semantically close within a sentence are not always structurally close within a sentence.

Overcome structural limits of language via attention.

We expect that introducing attention-mechanism to language-based inverse molecular design problems can help machines understand geometric structures of molecules beyond the limitations of chemical language itself. SMILES, a chemical language, represents molecules as one-dimensional text.

It is a powerful language since a one-SMILES string is converted into one exact molecule (see **SMILES language** in **Methods**). However, unfortunately, since most molecules are non-Hamiltonian graphs, it is self-evident that semantic discontinuity occurs whenever a branch in a molecule is translated into a one-dimensional string (**Fig. 1a**). SMILES distinguishes each branch with opening and closing round brackets, and it makes a gap between the distance of two characters within the string and the distance of corresponding two atoms in the molecular graph. An example is shown in **Fig. 1b**. Even though atom2 and atom13 in **Fig. 1b** are geometrically adjacent, these two atoms in the string are far from each other. In other words, the longer the branch is and the more branch is, the harder it is to imagine the molecular structure by reading the chemical string with your eyes in the order of it (like memory cells). A similar phenomenon occurs in natural language (**Fig. 1c**). The longer the sentence is, the bigger gap exists between the words within the sentence and the semantic similarity; unfortunately, in chemical language, there are more spots where semantic discontinuity occurs. In the field of NLP, by introducing attention-mechanism to this problem, language models were able to pay attention sparsely to find semantically related parts (see **Attention-mechanism** in **Methods**); it is a departure from the old way of perceiving context in the order of sentences (memory cells). Transformer is an architecture involving attention-mechanism in the form of a neural net, and it became a breakthrough in cognitive ability. We started our research with the expectation that attention-mechanism could help structural understanding beyond the semantic discontinuity of chemical language. The results and discussion on this will be covered in the later section (***How plausible are the generated molecules?***).

Machine learning model.

We designed GCT, an architecture that embeds Transformer—one of the most advanced language model—into a conditional variational autoencoder (cVAE)²⁸, which creates molecules with target

properties based on a deep understanding of chemical language. Transformer, the core of GCT's language recognition ability, is mainly used as a neural machine translator (NMT). It consists of an encoder and a decoder (**Fig 2.a**). The encoder receives a sentence to be translated and understands the received sentence through self-attention. Then, the processed information from sentence comprehension is passed to the decoder. The decoder iteratively selects the next word that will follow the translated sentence until now, referring to the information received from the encoder and the sentences translated up to the previous step; if there is no translated sentence at the beginning of translation, the special token 'start of sentence < sos >' is used. The decoder uses the input information to iteratively select the next word that will follow the translated sentence up to the previous step. Finally, the translation ends when the decoder selects a special token 'end of sentence < eos >'.

GCT is a structure that inserts a low-dimensional conditional Gaussian latent space between the encoder and the decoder of Transformer (**Fig. 2b**). The self-attention block of the encoder gets the concatenated array of the three different properties and SMILES string: octanol-water partition coefficient (logP), topological polar surface area (tPSA), and quantitative estimate of drug-likeness (QED)²⁹. The encoder-decoder attention block in the decoder gets the concatenated array of latent code and condition (three properties), and the self-attention block in the decoder gets the SMILES string only. In the training phase, GCT performs the task of reconstructing the SMILES string—input through the encoder—by referring to the given hints on molecular properties. In this process, the low-dimensional latent space acts as the model's bottleneck to find meaningful information that can be restored to the decoder as much as possible by exploiting the limited information passed through the bottleneck. Then, meaningful latent variables for molecular structures and properties are represented in low-dimensional continuous latent space. In the inference phase, a sampled latent code and target properties are input to the learned decoder, and the decoder selects the next tokens iteratively through 4-beam search; beam search is a kind of method for tree search. Other details about the model architecture and training methods are described in **Methods** and **Supplementary Information**.

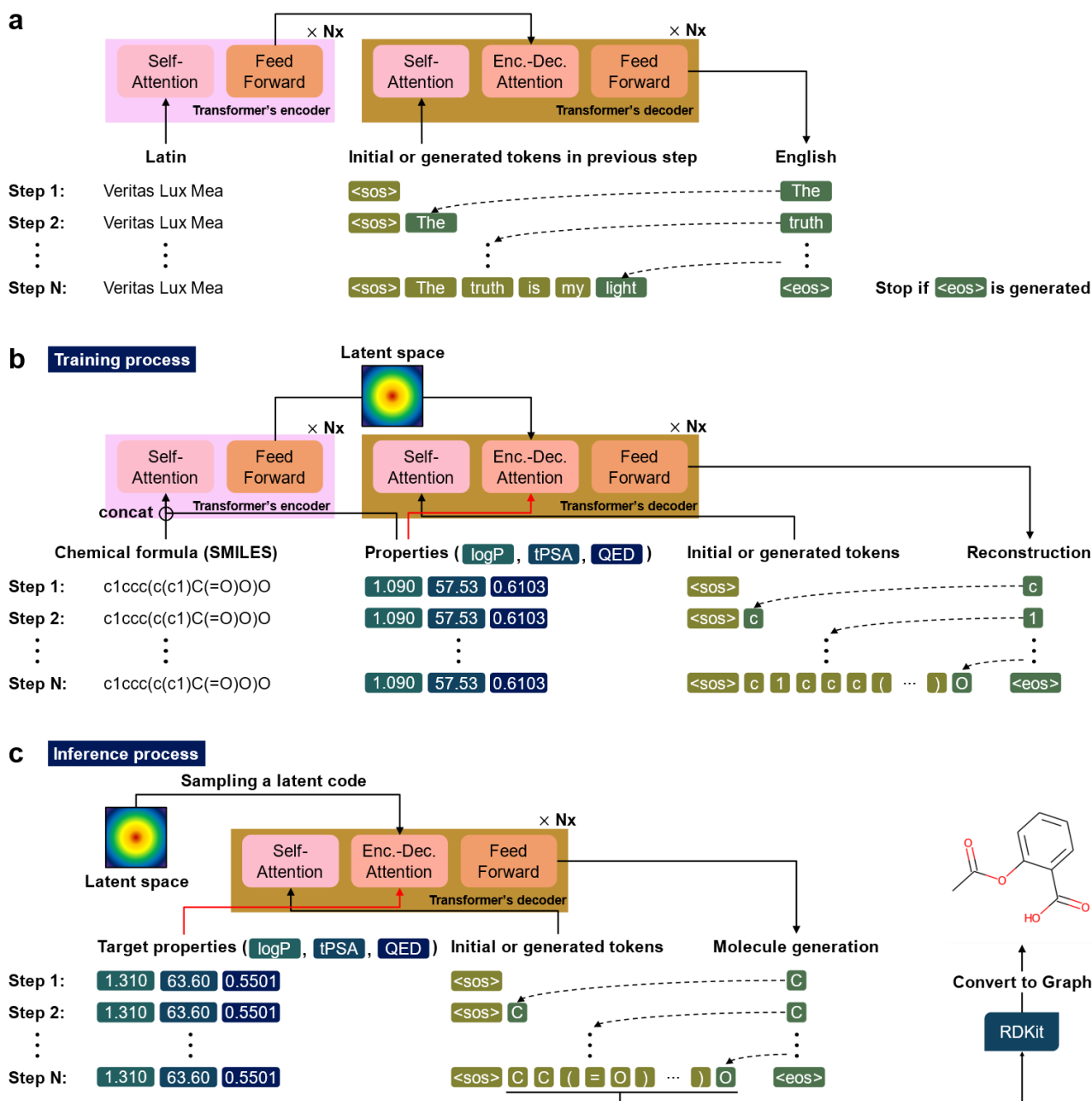


Fig. 2 De novo molecular generation via GCT. **a**, Transformer model for NMT: an example of translating Latin into English. It iteratively selects the next English word by referring to the Latin sentence and the English sentence translated up to the previous step. **b**, In the process of learning to reproduce the input chemical formula, GCT learns the molecular structure and three different properties: logP, tPSA, and QED. It represents the information of molecular structure and properties in the latent space during the learning process. **c**, The trained GCT generates a de novo molecule that satisfies the target properties by decoding the molecular information sampled from the latent space and the given preconditions.

Datasets & Benchmark.

GCT model was trained and benchmarked using a database of Molecular Sets (MOSES) benchmarking platform³⁰. MOSES database is a benchmarking dataset for drug discovery made by sampling molecules from ZINC database³¹—composed of commercially-available compounds—that satisfy specific conditions: weight in the range from 250 to 350 Daltons, the number of rotatable bonds not greater than 7, not containing charged atoms or atoms besides C, N, S, O, F, Cl, Br, H or cycles longer than 8 atoms. MOSES consists of training samples (1.7 M) and test samples (176 k), and scaffold test samples (176 k) which have scaffolds that never appear in the training samples. It is also designed to closely match the distribution between the datasets. We add three additional properties computed from RDKit³² to MOSES database and use them for the learning of GCT.

In general, the quality of network training can be evaluated by measuring how different the model's prediction and the actual label. However, for molecular generative models, the small mean loss does not guarantee that the generative model performs well. This is because the artifacts in the generated molecules, which are not observed in the mean loss measurement, may not fit the chemical valence rule or make the molecules unrealistic. For this reason, the quality of the generated molecules needs to be checked against the following criteria:

- How plausible are the generated molecules?
- Do the generated molecules satisfy the target properties?
- Can multiple candidates be generated for a single precondition set?
- Can create de novo molecules in a short time?

To answer the above criteria, the performance of GCT was quantitatively evaluated by benchmarking 30,000-generated molecules (**Table 1**). We divided the results and discussions into the criteria listed above and described each in the remaining sections.

Table 1 Comparison of MOSES benchmarking results

Conditional	Real molecule data (Sampled from ZINC ³¹)				Models						
	MOSES Test	MOSES Train	Ref. ³³	Relative error	Language-based					Graph- based	
					GCT (This work)	CharRNN ^{9,30}	AAE ^{30,34}	VAE ³⁰	Latent GAN ^{14,30}	JTN- VAE ^{30,35}	
					True	False					
Validity ^a	↑		1.0	1.0	0	0.9923	0.9748 ±0.0264	0.9368± 0.0341	0.9767 ±0.0012	0.8966 ±0.0029	1.0±0.0
Unique@1k ^b	↑		1.0	1.0	0	0.998	1.0±0.0	1.0±0.0	1.0±0.0	1.0±0.0	1.0±0.0
Unique@10k ^c	↑		1.0	0.9977	0.0023	0.9827	0.9994 ±0.0003	0.9973 ±0.002	0.9984 ±0.0005	0.9968 ±0.0002	0.9996 ±0.0003
IntDiv ^d	↑		0.8567	0.8678	0.0130	0.8462	0.8562 ±0.0005	0.8557 ±0.0031	0.8558 ±0.0004	0.8565 ±0.0007	0.8551 ±0.0034
Filters ^e	↑		1.0	0.6448	0.3552	0.9974	0.9943 ±0.0034	0.9960 ±0.0006	0.9970 ±0.0002	0.9735 ±0.0006	0.9760 ±0.0016
Novelty ^f	↑		1.0	0.9044	0.0956	0.6755	0.8419 ±0.0509	0.7931 ±0.0285	0.6949 ±0.0069	0.9498 ±0.0006	0.9143 ±0.0058
SNN ^g	↑	Test	0.6419	0.5201	0.1897	0.6510	0.6015 ±0.0206	0.6081 ±0.0043	0.6257 ±0.0005	0.5371 ±0.0004	0.5477 ±0.0076
		TestSF	0.5859	0.4918	0.1606	0.5999	0.5649 ±0.0142	0.5677 ±0.0045	0.5783 ±0.0008	0.5132 ±0.0002	0.5194 ±0.007
FCD ^h	↓	Test	0.008	7.5314	940.425	0.8224	0.0732 ±0.0247	0.5555 ±0.2033	0.0990 ±0.0125	0.2968 ±0.0087	0.3954 ±0.0234
		TestSF	0.4755	8.1312	16.1003	1.2668	0.5204 ±0.0379	1.0572 ±0.2375	0.5670 ±0.0338	0.8281 ±0.0117	0.9382 ±0.0531
Frag ⁱ	↑	Test	1.0	1.7705	0.7705	0.4487	0.9998 ±0.0002	0.9910 ±0.0051	0.9994 ±0.0001	0.9986 ±0.0004	0.9965 ±0.0003
		TestSF	0.9986	2.5697	1.5733	0.6412	0.9983 ±0.0003	0.9905 ±0.0039	0.9984 ±0.0003	0.9972 ±0.0007	0.9947 ±0.0002
Scaf ^j	↑	Test	0.9907	0.6720	0.3217	0.8558	0.9242 ±0.0058	0.9022 ±0.0375	0.9386 ±0.0021	0.8867 ±0.0009	0.8964 ±0.0039
		TestSF	0.0	0.1129	Inf.	0.0599	0.1101 ±0.0081	0.0789 ±0.009	0.0588 ±0.0095	0.1072 ±0.0098	0.1009 ±0.0105

MOSES benchmarking was performed on 30,000-SMILES strings generated by GCT. Then, the scores obtained from GCT were compared with the scores of models provided by MOSES benchmarking platform: CharRNN, AAE, VAE, LatentGAN, JTN-VAE. The upward arrow means that the higher value is the better and the downward arrow means that the lower value is the better. The relative error between the scores obtained from MOSES train data and the scores obtained from 30,000-molecules randomly sampled from ref. ³³'s train data. Both datasets are real molecule data sampled from ZINC. ^aThe ratio of valid SMILES strings. ^bThe ratio of unique samples out of 1,000-generated molecules. ^cThe ratio of unique samples out of 10,000-generated molecules. ^dThe Internal diversity of the generated molecules. ^eThe ratio of passing through toxic substance filters. ^fThe ratio of generated molecules that do not exist in the train data. ^gAverage of Tanimoto similarity for all generated molecules; the similarity between a generated molecule and the most similar molecule among the reference data is calculated. ^hMeasure the distance between the generated molecules and the reference molecules using the activations of the penultimate layer of ChemNet—bioactivity prediction model. ⁱThe cosine similarity between the frequency in which BRICS substructures appearing in the reference data and the frequency appearing in the generated molecules. ^jThe cosine similarity between the frequency in which specific scaffolds appearing in the reference data and the frequency appearing in the generated molecules.

How plausible are the generated molecules?

To evaluate whether the generated SMILES strings represent plausible molecular structures, analysis from two perspectives is required. The first is whether the generated SMILES strings can generate valid molecular graphs. In other words, it is whether the generated SMILES strings satisfy both the chemical valence rule and the syntax of SMILES language. Looking at the benchmarking results, it was found that 99.2% of the generated SMILES strings are valid, which is the highest value among language-based models (**Table 1a**). This ability depends on how well the generative machine can understand the geometry of molecules through SMILES strings. Because to determine the character (corresponding to atom, bond, or branch) followed by the given chemical string to satisfy the chemical valence rule and the grammar of SMILES language, the geometry of the molecules (connectivity of each atom and branches) present in the string must be understood. It is confirmed that attention-mechanism applied to GCT enables the neural machine to understand the molecular geometry beyond the semantic discontinuity of SMILES language. **Fig. 3** shows the results for two extreme examples of how GCT is paying attention to the characters within the SMILES string. The atom1,2 and atom13 in **Fig. 3a** are located close to each other on molecular graphs, however, far within the SMILES string. Although only SMILES string was provided to GCT, it is recognized that atom1,2 and atom13 are related to each other (♠); **Fig. 3b** shows that GCT recognizes the relationship between atom2 and atom22,23 (♦). It also recognizes atoms corresponding to a particular branch (♣) and recognizes the ring type of branch (♥). To sum up, we can confirm that GCT is well aware of the stereoscopic structure of molecules hidden in the one-dimensional text.

The second is how similar the molecular structures parsed from the valid SMILES strings are to real molecules. Four metrics can measure this: similarity to nearest neighbor (SNN)³⁰, Fréchet ChemNet distance (FCD)³⁶, fragment similarity (Frag)³⁰, and scaffold similarity (Scaf)³⁰. Among them, SNN is the most suitable metric for evaluating GCT (conditional generator). Because the distribution of molecules generated by conditional generators can be perturbed according to sampled condition sets,

a metric that can measure the similarity between the reference molecules and the generated molecules without considering the distribution or frequency of the molecules is required. SNN is a scoring metric that calculates the averaged similarity between all two molecules—one is a generated molecule and the other is the most similar molecule chosen in the reference set. Since SNN considers only two molecules, not the distribution or frequency, it is less sensitive to the distribution of the entire data and it is possible to measure how the tested molecule (generated molecule) is similar to a reference molecule (real molecule).

In contrast, the three other indicators are not suitable for evaluating the generated results of conditional generative models: FCD, Frag, and Scaf. Since these three indicators are very sensitive to the difference between the distribution of generated molecules and the distribution of reference molecules. It can be seen through the definition of each metric (see *MOSES benchmarking metrics* in **Methods**). The difference in distribution does not mean that the generated molecules derived by conditional generators are unrealistic or unplausible. To test this empirically, we calculated the score of FCD, Frag, and Scaf for the 30,000 molecules randomly sampled from ref. ³³'s train data. Although ref. ³³'s train data are composed of real molecules sampled from ZINC database like the MOSES database, due to the different distribution of the data, very bad scores for FCD, Frag, and Scaf are obtained. However, it was confirmed that the influence of the distribution difference was the least reflected in SNN (see the relative error column of **Table 1g-j**).

The comparative models provided by the MOSES benchmarking platform are non-conditional models specialized in an approximation of the train data's distribution; neural nets are high-performance universal approximators. It is possible to accurately follow the distribution of the train data by sampling the latent codes and decoding these. This is advantageous for non-conditional generative models to match the distribution of test data and the distribution of generated molecules since the MOSES benchmarking platform has constructed the datasets in a form that closely matches

the distribution of the train data and the test data. So, we used SNN to evaluate how well GCT generates molecules that are similar to real molecules compared to other comparative models.

GCT outperforms SNN scores for all compared models; the method used to set the conditions to generate molecules is written in *Condition sampling* in **Methods**. Furthermore, the generated molecules were very similar to real molecules, and hard to distinguish them (**Fig. 4** and **Fig. S2-11**). This is because the attention-mechanism of Transformer, which is the basis of GCT's comprehension ability, helps to learn molecular geometric structures from SMILES language by understanding the context and grammar. It also demonstrates that the relationship between molecular graphs and language is better inferred than memory cells such as long-short term memory (LSTM)³⁷ or gated recurrent unit (GRU)³⁸—methods of reading characters in order: LSTM (CharRNN^{9,30}), bidirectional LSTM (LatentGAN^{13,30}, AAE^{30,34}), and a combination of GRU and bidirectional GRU (VAE³⁰).

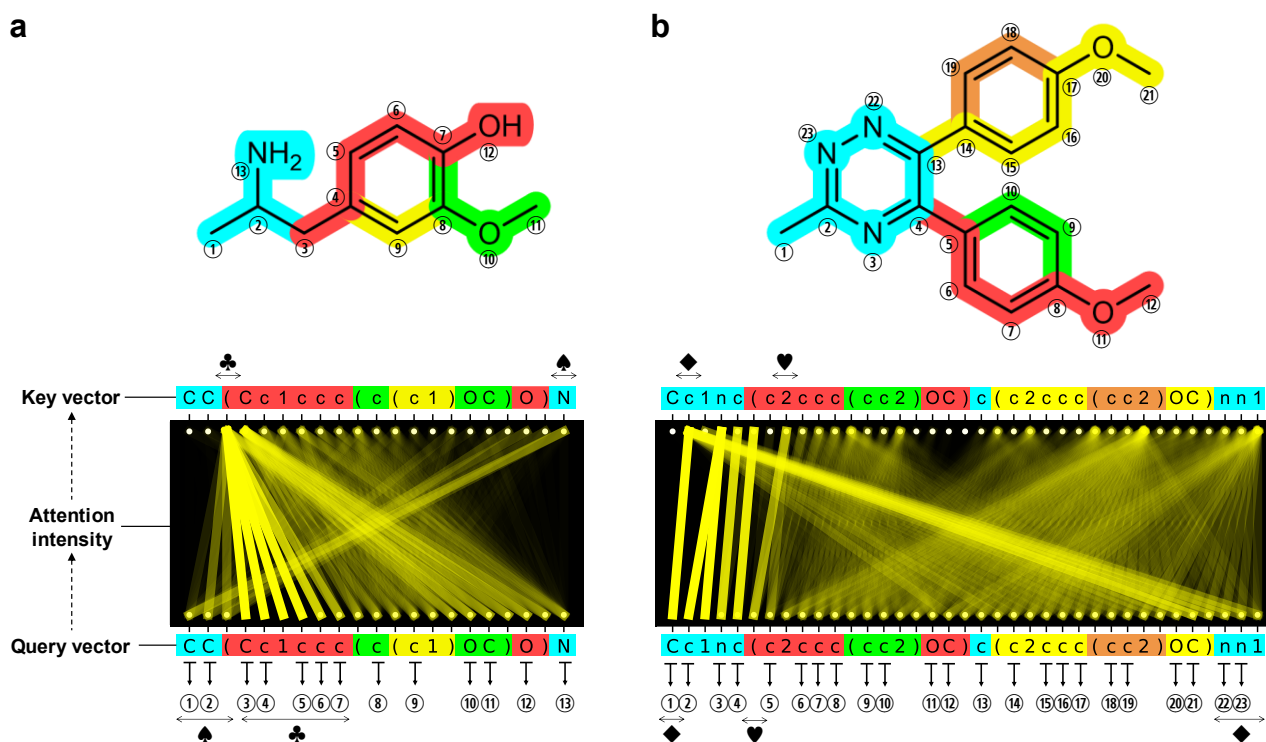


Fig. 3. Visualized examples for self-attention scores of an attention-head in encoder blocks. a, Visualization results of the fourth head in the second encoder block for 4-(2-Aminopropyl)-2-methoxyphenol. **b,**

Visualization results of the third head in the second encoder block for 5,6-bis(p-methoxyphenyl)-3-methyl-1,2,4-triazine. These are two extreme cases where the atom (atom13 in **a**, and atom23 in **b**) adjacent to atom2 on each molecular graph is represented far away on each SMILES string. GCT's encoder has six encoder blocks, each with eight attention-heads. Each head recognizes data from a different perspective. These are the results of picking and visualizing one attention-head for each. Attention intensity (yellow lines) is an expression of the attention score of each token in the Question vector paying attention to which tokens in the Key vector in the process of performing a given task. The more opaque the line is, the stronger attention is given between the two tokens. Each color colored on the SMILES string and the molecular graph represents each branch of the SMILES string separated with round brackets. The visualization scheme is borrowed from ref. 39.

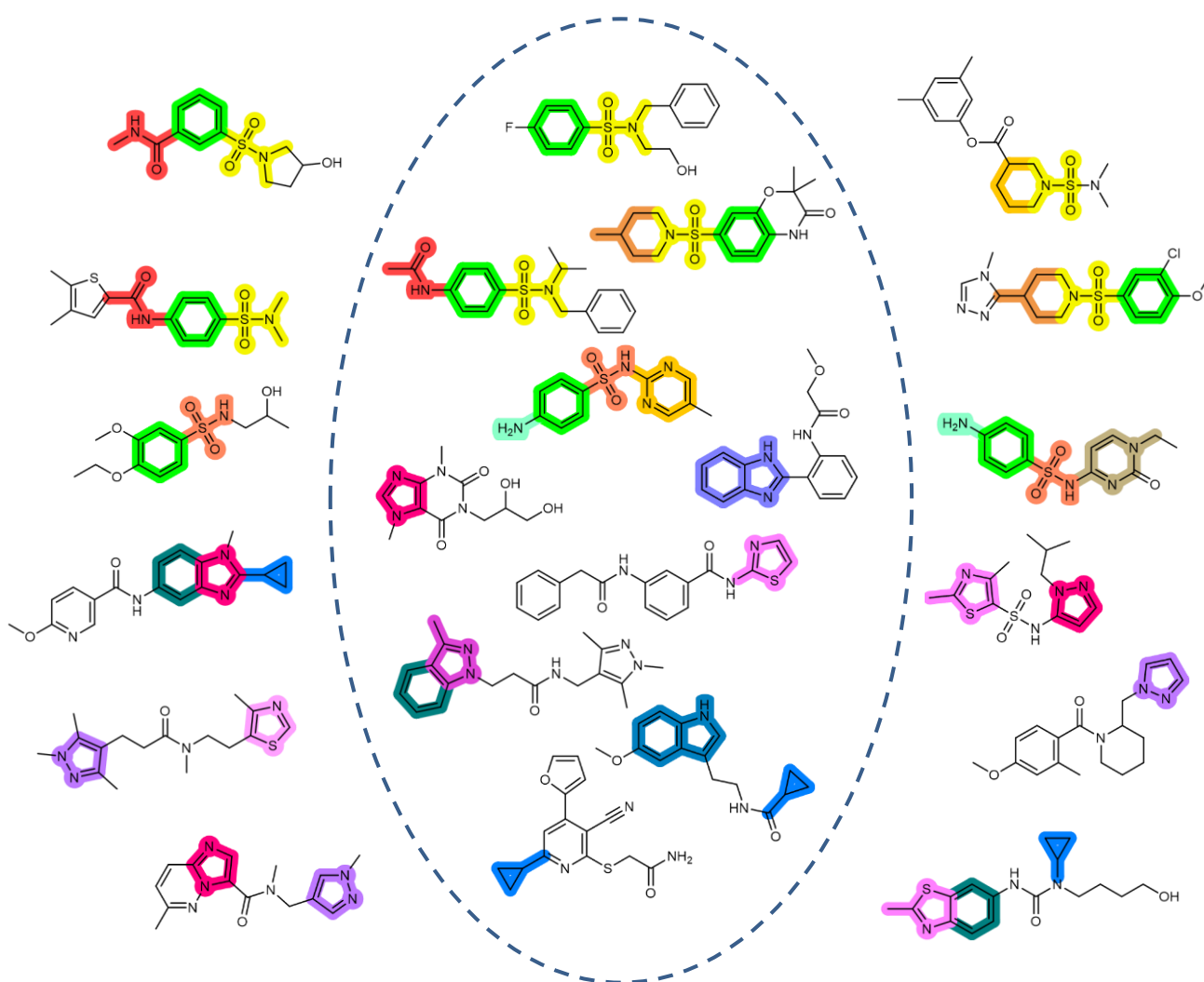


Fig. 4. Comparison of real molecules and generated molecules. The molecules in the dotted circle are real molecules, and the molecules outside the dotted circle are molecules generated by GCT. Similar substructures

of molecules are colored in similar color tones.

Do the generated molecules satisfy the target properties?

GCT generates molecular structures that satisfy the multiple target properties. **Fig. 5a-c** are the results of comparing the properties of 30,000-valid molecules generated from GCT (calculated from RDKit) and target properties (preconditions given in GCT). Since logP and tPSA are physical properties directly related to the molecular structure, it is possible to generate a molecular structure corresponding to the target property based on an understanding of the molecular structure. However, QED is an artificial index designed to determine the likeness to drugs quantitatively through geometric averages of eight different properties, so it is relatively difficult for QED; this aspect is also found in cRNNs. The absolute mean errors between the target conditions for each property and the properties of the generated molecule are 0.132 (logP), 0.193 (tPSA), and 0.020 (QED).

Another function of GCT is that it can control the length of the generated SMILES string by adjusting the length of the latent code. Since GCT has an autoencoder (AE) structure, it can reconstruct information input to the encoder. In the training phase, the length of the latent code appears equal to the length of the string input to the encoder and the length of the string output from the decoder; in fact, these are slightly different depending on whether <eos> and <eos> tokens are used in the input and output design; however, the nature of the string is not different (see **Supplementary Information**). Therefore, when generating molecules using the decoder, the number of tokens constituting the generated SMILES string can be controlled by adjusting the length of the latent code (**Fig. 5d**). It means that molecular size is controllable.

To check whether the given multiple target properties are satisfied simultaneously, the properties of generated molecules were compared to the 10-precondition sets which were sampled from the distribution of train data (**Fig. 5e-g**). The conditional model which is a skeleton of GCT well generates

molecules that simultaneously satisfy the multiple target properties. Furthermore, a variational generator in GCT makes it possible to generate various molecules under the same precondition set (Fig. S2-11).

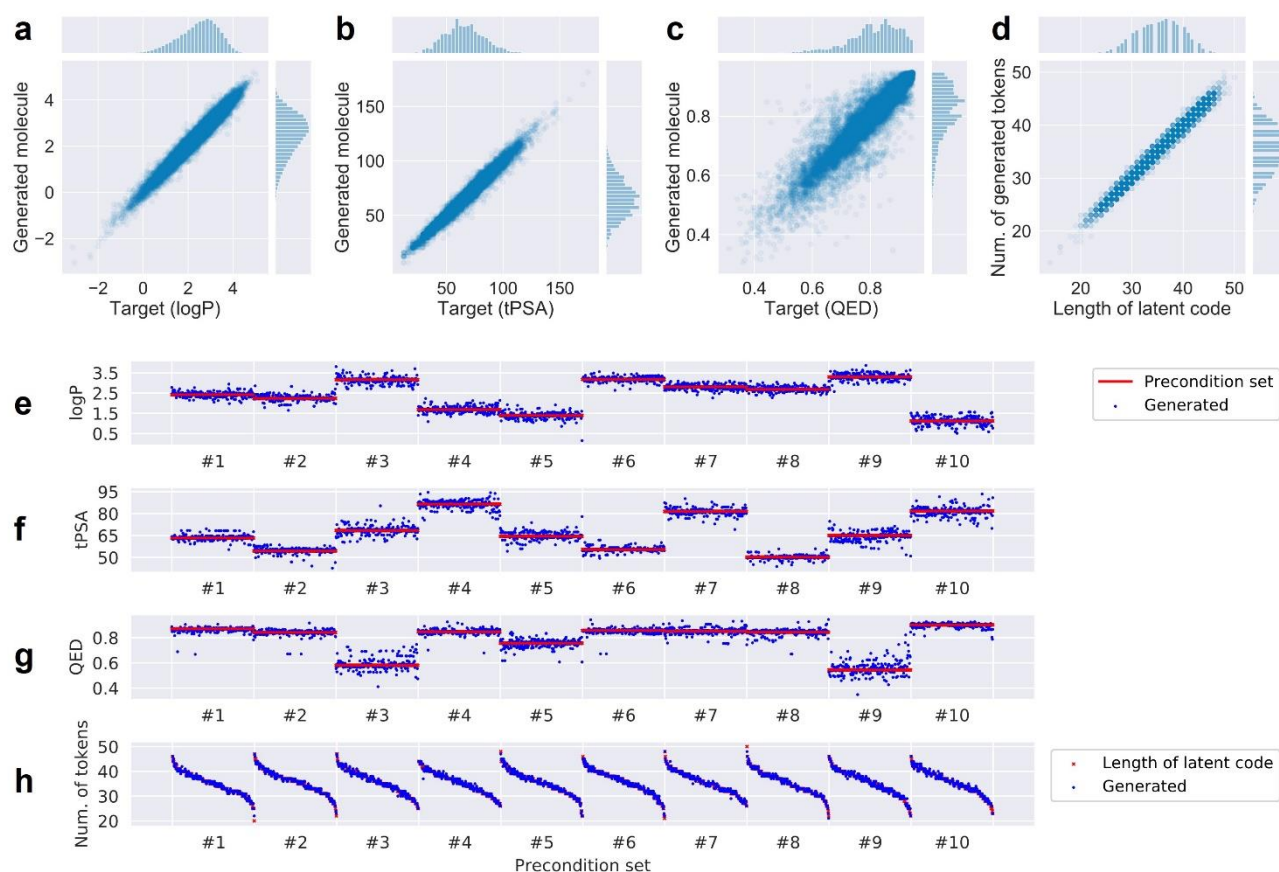


Fig. 5 Comparison of target properties (preconditions given to GCT) and properties of 30,000-generated molecules. a-c, The x-axis refers to the target property, and the y-axis refers to the property of the generated molecule. **d,** The x-axis refers to the length of the latent code, and the y-axis refers to the number of tokens constituting the generated SMILES string. **e-g,** 10-precondition sets randomly sampled from MOSES data distribution (red line) and properties of generated molecules (blue dot). **h,** The length of latent code randomly sampled from MOSES data distribution (red marker) and the number of tokens constituting of the generated molecule (blue dot).

Can create de novo molecules in a short time?

Whether a generative model can create de novo molecules is an important criterion that

determines its applicability as a tool for material discovery. The novelty score refers to the probability of generating a new molecule that does not exist in the train data (**Table 1f**). Note that just a high novelty score does not guarantee that it is a good generator. Odd and unrealistic molecules can increase the novelty score. Hence, the novelty score should be used in conjunction with indicators to evaluate whether the generated molecules are realistic. It is a difficult problem to create de novo molecules while maintaining common patterns of real molecules, even meets the multiple desired conditions simultaneously. GCT has a relatively low 67.6% probability of generating a new molecule. However, it is sufficiently usable level, and the qualitative level of the generated molecules is quite high; the generated molecules are realistic and controllable.

GCT can generate de novo molecules in a sufficiently short time at a personal computer level. The time taken per molecule generation was 507 ms in the environment of 8C/16T CPU and GTX1080Ti; 440 ms with 12C/24T and Tesla T4. This is an impossibly short time for human experts to use their knowledge to design a new molecule. It means that it can be used as a tool to accelerate material discovery.

Conclusions

In this study, we proposed GCT architecture that embeds Transformer—a language model that has been a breakthrough in the field of NLP using attention-mechanism—into a conditional variational generator. Learned GCT can generate SMILES strings that meet the desired conditions based on a deep understanding of chemical language. It learned molecular structures and three different properties as a form of language: logP, tPSA, and QED. Quantitative evaluations were performed by scoring molecules converted from the generated SMILES strings. In this process, the characteristics of the indicators (SNN, FCD, Frag, and Scaf) that measure the reality of the molecules were analyzed and the limitations were discussed. And the performance of GCT was benchmarked by MOSES

benchmarking platform. By analyzing the results, we concluded the effects of utilizing language models on inverse molecular design problems. We demonstrated that GCT can utilize both the advantages of a language model and a conditional variational generator. Summarizing the conclusions obtained are as follows:

- (1) Attention-mechanism in GCT helps to deeply understand the geometric structure of molecules beyond the limitations of chemical language—semantic discontinuity resulting from converting a non-Hamiltonian molecular graph as a one-dimensional string—by sparsely paying attention to chemical formulas.
- Deep understanding of chemical language makes the generated SMILES strings (2) satisfy the syntax of SMILES language, (3) satisfy the chemical rules, and (4) be realistic.
- Conditional variational generator in GCT makes the generated molecules (5) satisfy multiple target properties simultaneously, and (6) be various.
- AE in GCT (7) makes the molecular size controllable.
- GCT (8) creates de novo molecules that have never been seen in the training process, and (9) creates molecules in a short time that human experts cannot.

GCT generates valid SMILES strings with 99.2% probability, and the SNN score obtained from the generated molecules was 0.651. This is the highest validity among the compared language-based generative models, and the SNN score is the highest value compared to the scores of all the compared generative models including the graph-based approach. Also, the generated molecules satisfied multiple target properties simultaneously, and the mean absolute error for three different properties were 0.132 (logP), 0.193 (tPSA), and 0.020 (QED). Besides, it was confirmed that GCT can control the molecular size; the averaged difference in the number of generated SMILES tokens compared to the given length of latent code is 0.382. Molecular generation took 507 ms per molecule at the personal

computer level, which is an impossibly short time for human experts to do. Furthermore, conditions applicable to GCT can be configured differently as needed, and GCT can be extended to Transformer-based architectures such as BERT⁴⁰, GPT⁴¹, and T5⁴². Considering the time required versus the advantages listed above, it is expected that our proposed model can contribute to accelerating the process of material discovery.

Methods

SMILES language.

SMILES expresses the atoms, bonds, and rings that make up molecules as a string. Atom is represented by the alphabet of the element symbol, and bond is represented by a single bond (-), double bonds (=), and triple bonds (#), depending on the type. In general, a bond that can be easily inferred through the atoms or ring structure of the surrounding atom is omitted. For charged atoms, where the number of hydrogen bonds cannot be determined explicitly, atoms and formal charges are written together in the bracket []. The beginning and end of each ring are expressed in the same digit, and the pair must be correct; if a ring is open, it must be closed. The atoms present in the aromatic ring are written in lowercase, while the atoms outside are capitalized (see **Fig. 1b**).

Tokenization and token embedding.

To input SMILSE string to language models, the process of tokenizing by semantic units is necessary. The SmilesPE⁴³ tokenizer was used to tokenize the SMILSE strings included in the MOSES train data. There are a total of 28 types of tokens used: 4-special token (<unknown>, <pad>, <sos>, <eos>), 13-atom token (<C>, <c>, <O>, <o>, <N>, <n>, <F>, <S>, <s>, <Cl>,
, <[nH]>, <[H]>), 3-bond tokens (<->, <=>, <#>), 2-branch token (<(>, <)>), 6-ring token (<1>, <2>, <3>, <4>, <5>, <6>). For this reason, each token that constitutes SMILES string is one-hot encoded in 28-dimension and is

embedded in 512-dimension. The condition of GCT is also embedded in 512 dimensions.

Attention-mechanism.

Attention-mechanism is the core of Transformer's language cognitive abilities. Attention-mechanism allows Transformer to self-learn which token of the input string is better to focus on to perform a given task better. Attention-mechanism uses three vectors: Query Q , Key K , Value V . Information of the hidden state is expressed in Q . Network finds keys in Q that can express Q well and derives an attention score by reflecting the corresponding V ; if the first layer, Q refers input data. There are many ways to implement attention-mechanism, and Transformer uses scaled dot-product attention:

$$Attention(Q, K, V) = softmax\left(\frac{QK^T}{\sqrt{d_k}}\right)V \quad (1)$$

where d_k means the dimension of the K , and d_k must correspond to the dimension d_q of the Q .

Conditional variational transformer.

The structure of GCT is designed to add a conditional Gaussian latent space between the encoder and the encoder of the Pre-layer normalization (Pre-LN) Transformer²⁷. Pre-LN Transformer is a modified version of the well-known (Post-layer normalization, Post-LN) Transformer²⁵. The combination of language models and variational autoencoders is vulnerable to posterior collapse⁴⁴, which can be mitigated by 48, KL-annealing. A complete solution to posterior collapse has yet to be identified, however, KL-annealing can alleviate it⁴⁵. Since KL-annealing is a method of controlling gradient size, adopting Pre-LN Transformer—designed to stabilize the gradient flow of (Post-LN) Transformer—can facilitate KL-annealing manipulation. The loss function of GCT is as follows:

$$L(\phi, \theta; x_{enc}, x_{<t}, x_t, c) = -k_w D_{KL}(q_\phi(z|x_{enc}, c) \parallel p(z|c)) + E_{q_\phi(z|x_{enc}, c)}[\log g_\theta(x_t|z, x_{<t}, c)] \quad (2)$$

where ϕ , θ , x_{enc} , $x_{<t}$, z , x_t , and c are the parameter set of the encoder, the parameter set of the decoder, the input of the encoder, the input of the decoder, the latent variables, the target to reconstruct, and the conditions, respectively. $D_{KL}(\cdot)$ is KL-divergence, and $E[\cdot]$ is the expectation of \cdot . q_ϕ is parameterized encoder function, g_θ is parameterized decoder function (generator), and $p(\cdot|c)$ is conditional Gaussian prior. k_w is the weight for KL-annealing. Encoder and decoder each consist of six Pre-LN Transformer blocks. The block has a dimension of 512, 8-head attention, and the dimension of the feed-forward block is 2,048. The Gaussian latent space is designed in 128-dimension. Dropout is 0.3 applied. Learning is conducted by Adam optimizer⁴⁶. Learning rates are scheduled using a one-epoch cycle of stochastic gradient descents with warm starts (SGDR)⁴⁷. The initial learning rate is 10^{-4} , the expansion rate of momentum is 0.9 and the expansion rate of the adaptive term is 0.98. KL-annealing was applied to grow k_w from 0.00 to 0.50 at 0.02 intervals per epoch, and for a total of 26 epochs. Other details of GCT are provided in **Supplementary Information**.

MOSES benchmarking metrics

30,000-SMILES strings are generated by learned GCT and benchmarked. In addition to relatively simple scores such as validity, uniqueness, internal diversity, filters, and novelty, MOSES benchmarking platform also provides metrics that can measure similarity with reference molecules such as SNN, FCD, Frag, and Scaf. However, some of them also yield similarity by measuring the distribution differences between two sets, which are not suitable for evaluating models that can perturb the distribution of generated data according to the given condition, such as the conditional generative model. SNN score is calculated as equation (2)³⁰:

$$SNN(G, R) = \frac{1}{|G|} \sum_{m_G \in G} \max_{m_R \in R} T(m_G, m_R) \quad (2)$$

where G and R refer to the set of molecules generated and reference molecules, respectively. m

stands for Morgan fingerprints⁴⁸, and $T(A, B)$ stands for Tanimoto similarity⁴⁹ between set A and set B . Since SNN is calculated as Tanimoto similarity between two molecules. One is a molecule to be tested and the other one is the most similar molecule in reference data. Although affected by the distribution of reference data, it is relatively insensitive to distribution compared to other similarity measure metrics. This is because rather than comparing the overall distribution or frequency of the generated molecules, one is selected and compared with the most similar one in reference samples. This can also be seen in the relative error column of **Table 1**.

FCD uses activation of the penultimate layer in ChemNet, designed to predict bioactivity. It calculates the difference of distribution between G and R as equation (3)³⁰:

$$FCD(G, R) = \|\mu_G - \mu_R\|^2 + Tr \left(\sum_G + \sum_R - 2 \left(\sum_G \sum_R \right)^{1/2} \right) \quad (3)$$

where μ is the mean, Σ is the covariance, and $Tr(\cdot)$ is the trace operator. FCD is highly sensitive to the distribution of data, as shown by the results of the original paper (ref. ³⁶). It outputs a very bad score even for real molecules which shows a different distribution. For conditional generators, the distribution of G depends on the sampling conditions. Hence, it is not appropriate to apply this metric to GCT.

Frag score is calculated as equation (4)³⁰:

$$Frag(G, R) = \frac{\sum_{f \in F} (c_f(G) \cdot c_f(R))}{\sqrt{\sum_{f \in F} c_f^2(G)} \sqrt{\sum_{f \in F} c_f^2(R)}} \quad (4)$$

where F is the set of 58,315 unique BRICS fragments⁵⁰, and $C_f(A)$ is the frequency with which fragment $f \in F$ appears in the molecules in set A .

Scaf score is calculated as equation (5)³⁰:

$$Scaf(G, R) = \frac{\sum_{s \in S} (c_s(G) \cdot c_s(R))}{\sqrt{\sum_{s \in S} c_s^2(G)} \sqrt{\sum_{s \in S} c_s^2(R)}} \quad (5)$$

where S is the set of 448,854 unique Bemis-Murcko scaffolds⁵¹, and $C_s(A)$ is the frequency with which scaffold $s \in S$ appears in the molecules in set A . Frag and Scaf derive the similarity with the same way of a well-known method in text mining: cosine similarity between the frequencies in which specific words appear in sentences belonging to each document to measure the similarity of two documents. However, this metric has the characteristic that the degree of similarity changes when the distribution of data (a genre of a document) changes. Hence, the low similarity between two real documents does not imply that the tested document is unreal. That is, these are metrics that measure the difference in distribution, and are not suitable for evaluating models that can perturb the distribution of generated data such as GCT.

Condition sampling.

Some of the metrics provided by MOSES benchmarking are sensitive to the distribution of the data, as discussed above. For this reason, the scoring value varied greatly depending on the sampling method. The benchmarking results obtained in this work were made for molecules generated through the condition sampling method as follows. The properties considered in this problem are logP, tPSA, and QED. A three-dimensional histogram was derived after equally dividing each property into 1,000 sections between the maximum and minimum values in the train data. Then, cells were sampled according to the probability that data samples exist in each cell; here, the probability is the number of samples in that cell of the total samples. Next, uniform noise was added at the center value of the cell to create condition sets for 30,000 molecules to be generated; the size of each uniform noise for logP-axis, tPSA-axis, and QED-axis is applied not to exceed the size of cell sides in each axis direction. This method approximates the distribution of the train data to some extent to obtain a good score compared to the uniform or normal sampling, however, it is hard to show the approximation performance as well as the complex neural net.

References

1. Virshup, A. M., Contreras-García, J., Wipf, P., Yang, W. & Beratan, D. N. Stochastic voyages into uncharted chemical space produce a representative library of all possible drug-like compounds. *Journal of the American Chemical Society* **135**, 7296-7303 (2013).
2. Daylight Chemical Information Systems, Inc.: SMARTS; <https://www.daylight.com/dayhtml/doc/theory/theory.smarts.html>
3. Heller, S. R., McNaught, A., Pletnev, I., Stein, S. & Tchekhovskoi, D. InChI, the IUPAC International Chemical Identifier. *Journal of Cheminformatics* **7** (2015).
4. Weininger, D. SMILES, a chemical language and information system. 1. Introduction to methodology and encoding rules. *Journal of Chemical Information and Modeling* **28**, 31-36 (1988).
5. Weininger, D., Weininger, A. & Weininger, J. L. SMILES. 2. Algorithm for generation of unique SMILES notation. *Journal of Chemical Information and Modeling* **29**, 97-101 (1989).
6. Weininger, D. SMILES. 3. DEPICT. Graphical depiction of chemical structures. *Journal of Chemical Information and Modeling* **30**, 237-243 (1990).
7. Arús-Pous, J. et al. Randomized SMILES strings improve the quality of molecular generative models. *Journal of Cheminformatics* **11** (2019).
8. Amabilino, S., Pogány, P., Pickett, S. D. & Green, D. V. S. Guidelines for recurrent neural network transfer learning-based molecular generation of focused libraries. *Journal of Chemical Information and Modeling* **60**, 5699-5713 (2020).
9. Segler, M. H. S., Kogej, T., Tyrchan, C. & Waller, M. P. Generating focused molecule libraries for drug discovery with recurrent neural networks. *ACS Central Science* **4**, 120-131 (2018).

10. Kingma, D. P. & Welling, M. Auto-Encoding Variational Bayes. Preprint at <https://arxiv.org/abs/1312.6114> (2014).
11. Gómez-Bombarelli, R. et al. Automatic Chemical Design Using a Data-Driven Continuous Representation of Molecules. *ACS Central Science* **4**, 268-276 (2018).
12. Blaschke, T. et al. Application of generative autoencoder in de novo molecular design. Preprint at <https://arxiv.org/abs/1711.07839> (2017).
13. Goodfellow, I. J. et al. Generative Adversarial Networks. Preprint at <https://arxiv.org/abs/1406.2661> (2014).
14. Prykhodko, O. et al. A de novo molecular generation method using latent vector based generative adversarial network. *Journal of Cheminformatics* **11** (2019).
15. Olivecrona, M., Blaschke, T., Engkvist, O. & Chen, H. Molecular de-novo design through deep reinforcement learning. *Journal of Cheminformatics* **9** (2017).
16. Griffiths, R.-R. & Hernández-Lobato, J. M. Constrained Bayesian optimization for automatic chemical design using variational autoencoders. *Chemical Science* **11**, 577-586 (2020).
17. Winter, R. et al. Efficient multi-objective molecular optimization in a continuous latent space. *Chemical Science* **10**, 8016-8024 (2019).
18. Janet, J. P., Chan, L. & Kulik, H. J. Accelerating Chemical Discovery with Machine Learning: Simulated Evolution of Spin Crossover Complexes with an Artificial Neural Network. *The Journal of Physical Chemistry Letters* **9**, 1064-1071 (2018).
19. Moosavi, S. M. et al. Capturing chemical intuition in synthesis of metal-organic frameworks. *Nature Communications* **10** (2019).
20. Nigam, A., Friederich, P., Krenn, M. & Aspuru-Guzik, A. a. Augmenting Genetic Algorithms

- with Deep Neural Networks for Exploring the Chemical Space. Preprint at <https://arxiv.org/abs/1909.11655> (2020).
21. Yang, X., Zhang, J., Yoshizoe, K., Terayama, K. & Tsuda, K. ChemTS: an efficient python library for de novo molecular generation. *Science and Technology of Advanced Materials* **18**, 972-976, doi:10.1080/14686996.2017.1401424 (2017).
 22. Segler, M. H. S., Preuss, M. & Waller, M. P. Planning chemical syntheses with deep neural networks and symbolic AI. *Nature* **555**, 604-610 (2018).
 23. Zhang, X., Zhang, K. & Lee, Y. Machine Learning Enabled Tailor-Made Design of Application-Specific Metal–Organic Frameworks. *ACS Applied Materials & Interfaces* **12**, 734-743 (2020).
 24. Kotsias, P.-C. et al. Direct steering of de novo molecular generation with descriptor conditional recurrent neural networks. *Nature Machine Intelligence* **2**, 254-265 (2020).
 25. Vaswani, A. et al. Attention Is All You Need. In *proceedings of the 31st International Conference on Neural Information Processing Systems*, 6000-6010 (2017).
 26. Bahdanau, D., Cho, K. H. & Bengio, Y. Neural Machine Translation by Jointly Learning to Align and Translate. In *proceedings of 3rd International Conference on Learning Representations* (2015).
 27. Xiong, R. et al. On layer normalization in the transformer architecture. In *proceedings of International Conference on Machine Learning* 10524-10533 (2020).
 28. Sohn, K., Lee, H. & Yan, X. Learning structured output representation using deep conditional generative models. *Advances in neural information processing systems* **28**, 3483-3491 (2015).
 29. Bickerton, G. R., Paolini, G. V., Besnard, J., Muresan, S. & Hopkins, A. L. Quantifying the chemical beauty of drugs. *Nature Chemistry* **4**, 90-98 (2012).

30. Polykovskiy, D. et al. Molecular sets (MOSES): a benchmarking platform for molecular generation models. *Frontiers in pharmacology* **11** (2020).
31. Sterling, T. & Irwin, J. J. ZINC 15 – Ligand Discovery for Everyone. *Journal of Chemical Information and Modeling* **55**, 2324-2337 (2015).
32. Landrum, G. et al. RDKit: Open-Source Cheminformatics Software (2019); <https://www.rdkit.org/>.
33. Ryu, S., Lim, J., Hong, S. H. & Kim, W. Y. Deeply learning molecular structure-property relationships using attention-and gate-augmented graph convolutional network. *Preprint at <https://arxiv.org/abs/1805.10988>* (2018).
34. Kadurin, A. et al. The cornucopia of meaningful leads: Applying deep adversarial autoencoders for new molecule development in oncology. *Oncotarget* **8**, 10883-10890 (2017).
35. Jin, W., Barzilay, R. & Jaakkola, T. Junction tree variational autoencoder for molecular graph generation. In *Proceedings of International Conference on Machine Learning*. 2323-2332 (2018).
36. Preuer, K., Renz, P., Unterthiner, T., Hochreiter, S. & Klambauer, G. Fréchet ChemNet Distance: A Metric for Generative Models for Molecules in Drug Discovery. *Journal of Chemical Information and Modeling* **58**, 1736-1741 (2018).
37. Hochreiter, S. & Schmidhuber, J. Long Short-Term Memory. *Neural Computation* **9**, 1735-1780 (1997).
38. Cho, K. et al. Learning Phrase Representations using RNN Encoder–Decoder for Statistical Machine Translation. In *Proceedings of the Conference on Empirical Methods in Natural Language Processing*. 1724-1734 (2014).
39. Vig, J. A multiscale visualization of attention in the transformer model. *Preprint at*

- <https://arxiv.org/abs/1906.05714> (2019).
40. Devlin, J., Chang, M.-W., Lee, K. & Toutanova, K. BERT: Pre-training of deep bidirectional Transformers for language understanding. *Preprint at <https://arxiv.org/abs/1810.04805>* (2019).
 41. Brown, T. B. et al. Language models are few-shot learners. *Preprint at <https://arxiv.org/abs/2005.14165>* (2020).
 42. Raffel, C. et al. Exploring the Limits of Transfer Learning with a Unified Text-to-Text Transformer. *Journal of Machine Learning Research* **21**, 1-67 (2020).
 43. Li, X. & Fourches, D. SMILES Pair Encoding: A Data-Driven Substructure Tokenization Algorithm for Deep Learning. Preprint at <https://doi.org/10.26434/chemrxiv.12339368.v1> (2020).
 44. He, J., Spokoyny, D., Neubig, G. & Berg-Kirkpatrick, T. Lagging Inference Networks and Posterior Collapse in Variational Autoencoders. In *proceedings of 7th International Conference on Learning Representations (2019)*.
 45. Samuel, R. B. et al. Generating Sentences from a Continuous Space. *Preprint at <https://arxiv.org/abs/1511.06349>* (2016).
 46. Kingma, D. P. & Ba, J. Adam: A Method for Stochastic Optimization. In *proceedings of 3th International Conference on Learning Representations (2015)*.
 47. Loshchilov, I. & Hutter, F. SGDR: Stochastic Gradient Descent with Warm Restarts. In *proceedings of 5th International Conference on Learning Representations (2017)*.
 48. Rogers, D. & Hahn, M. Extended-Connectivity Fingerprints. *Journal of Chemical Information and Modeling* **50**, 742-754 (2010).
 49. Tanimoto, T. T. Elementary mathematical theory of classification and prediction. *IBM Internal Report (1958)*.

50. Degen, J., Wegscheid-Gerlach, C., Zaliani, A. & Rarey, M. On the Art of Compiling and Using 'Drug-Like' Chemical Fragment Spaces. *ChemMedChem* **3**, 1503-1507 (2008).
51. Bemis, G. W. & Murcko, M. A. The Properties of Known Drugs. 1. Molecular Frameworks. *Journal of Medicinal Chemistry* **39**, 2887-2893 (1996).

Supplementary Information for manuscript

Generative chemical transformer: attention makes neural machine learn molecular geometric structures via text

Hyunseung Kim[†], Jonggeol Na^{‡,*}, Won Bo Lee^{†,*}

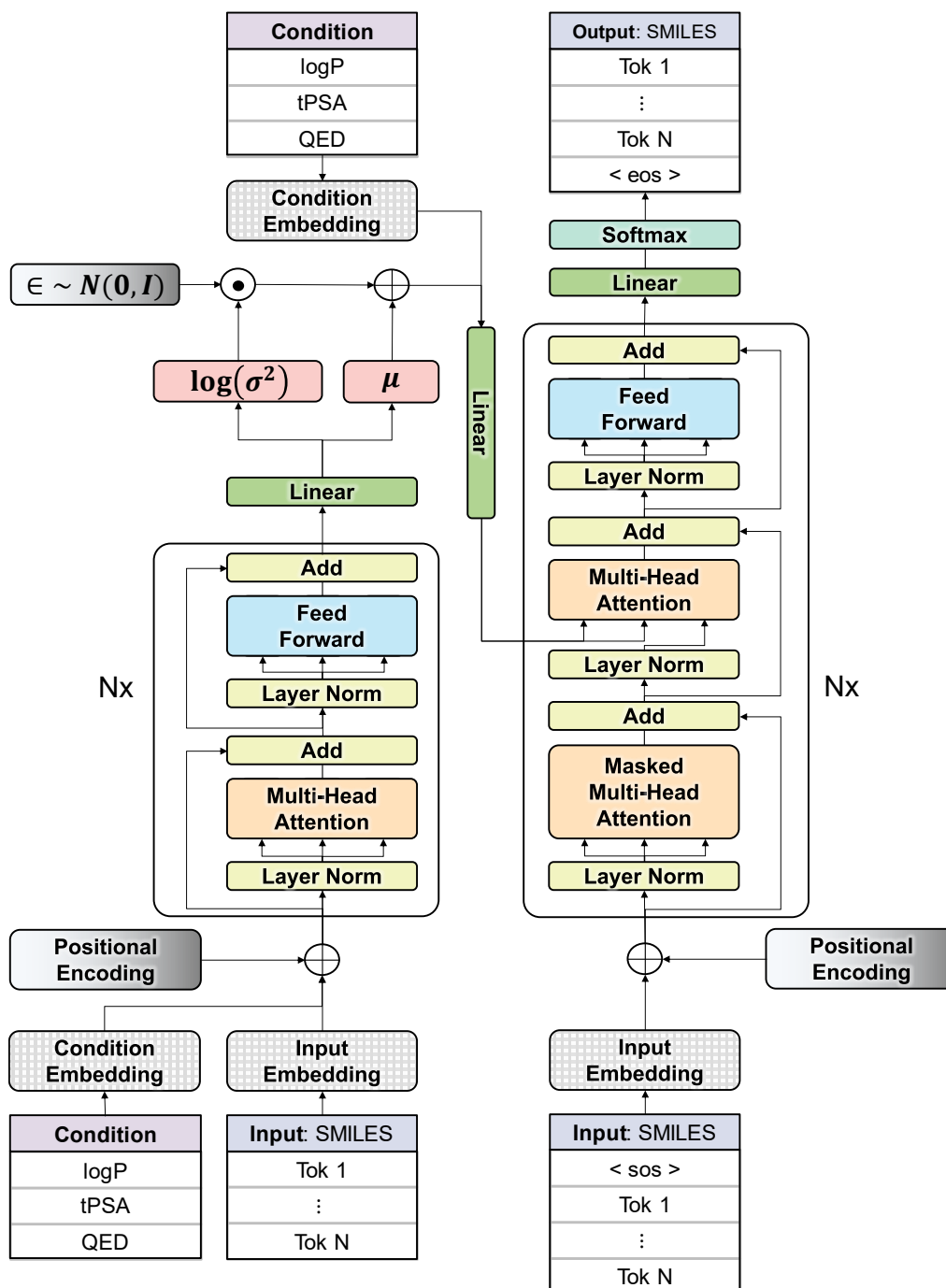
[†]School of Chemical and Biological Engineering, Seoul National University, Gwanak-ro 1, Gwanak-gu, Seoul 08826, Republic of Korea

[‡]Division of Chemical Engineering and Materials Science, Ewha Womans University, Seoul 03760, Republic of Korea

Correspondence and requests for materials should be addressed to

W.B.L. (email: wblee@snu.ac.kr) or J.N. (email: jgna@ewha.ac.kr).

The architecture of conditional variational Transformer (cVT)



Supplementary Figure 1. The architecture of conditional variational Transformer.

Supplementary Figure 1 shows the network architecture of cVT. Since cVT is based on the structure of conditional variational autoencoder (cVAE)¹, it is trained in the form of reconstructing information that enters the encoder through the decoder. The encoder receives a tokenized SMILES

string and three different properties: logP, tPSA, and QED. First, the tokenized SMILES string is one-hot encoded for 26 types of tokens: : <unknown>, <pad>, <C>, <c>, <O>, <o>, <N>, <n>, <F>, <S>, <s>, <Cl>,
, <[nH]>, <[H]>, <->, <=>, <#>, <(,>, <,>, <1>, <2>, <3>, <4>, <5>, <6>. The maximum length of the tokenized string is set to 80. The empty part is filled with <pad> token. Each token is then embedded into 512 dimensions which is the same as the model dimension. The conditions entered in the encoder are also embedded in 512 dimensions and concatenated in the embedded SMILES string; the conditions are placed in front and the SMILES string is attached to the back. The dimension entered the encoder block is then $R^{(3+80)\times 512}$.

The language model applied to cVT is pre-layer normalization (pre-LN) Transformer². The encoder has six pre-LN encoder blocks. The encoder has 8 multi-head attention, each head has 64 dimensions. Information on the properties and molecular structures leaving the Encoder is represented to the 128-dimensional conditional Gaussian latent space. Latent code sampled from latent space is concatenated with the target condition; the conditions are placed in front and the latent code is attached to the back. Then, the concatenated array expanded to 512 dimensions is entered into the encoder-decoder attention block of the decoder.

The decoder has two inputs; One is the concatenated array described above and the other input is the SMILES string generated up to the previous step. The latter is entered in the self-attention block of decoder, after one-hot encoding for 28 types of tokens: <unknown>, <sos>, <eos>, <pad>, <C>, <c>, <O>, <o>, <N>, <n>, <F>, <S>, <s>, <Cl>,
, <[nH]>, <[H]>, <->, <=>, <#>, <(,>, <,>, <1>, <2>, <3>, <4>, <5>, <6>. The information entered in this way passes through six pre-LN decoder blocks and exits the decoder. The array that leaves the decoder is reduced to the same dimension as the one-hot encoded tokens, and then softmax is taken to select the next one token that will come after the string entered in the decoder's self-attention block.

<sos> and <eos> tokens are only added to the SMILES string which is input and output to the decoder; the SMILES string input to the encoder does not have <sos> and <eos> tokens. There are two

reasons why we designed it like this. The first is that the dimension of conditions is constant, so if the SMILES string is put behind the conditions, the location of the beginning and end of the SMILES string within the concatenated input array can be recognizable. The second is the irrationality that can occur during latent code sampling. Using tokens with $\langle \text{sos} \rangle$ and $\langle \text{eos} \rangle$ can cause problems when sampling the latent code of $\langle \text{sos} \rangle$ and $\langle \text{eos} \rangle$ token location; the location where $\langle \text{sos} \rangle$ appears is always constant and it cannot be randomly sampled. For this reason, $\langle \text{sos} \rangle$ and $\langle \text{eos} \rangle$ are not used in the SMILES string entered in the encoder.

The loss function of cVT training is given as follows:

$$L(\emptyset, \theta; x_{enc}, x_{<t}, x_t, c) = -k_w D_{KL}(q_\emptyset(z|x_{enc}, c) \parallel p(z|c)) + E_{q_\emptyset(z|x_{enc}, c)}[\log g_\theta(x_t|z, x_{<t}, c)] \quad (1)$$

where \emptyset , θ , x_{enc} , $x_{<t}$, z , x_t , and c are the parameter set of the encoder, the parameter set of the decoder, the input of the encoder, the input of the decoder, the latent variables, the target to reconstruct, and the conditions, respectively. $D_{KL}(\cdot)$ is KL-divergence, and $E[\cdot]$ is the expectation of \cdot . q_\emptyset is parameterized encoder function, g_θ is parameterized decoder function (generator), and $p(\cdot|c)$ is conditional Gaussian prior. k_w is the weight for KL-annealing. The first term in Equation (1) is a term that forces the distribution of the encoder's output to follow the conditional Gaussian prior. The second term is a term to reconstruct the target that will come after the string entered in the decoder's self-attention block using z, c , and $x_{<t}$. Learning was carried out in teacher forcing manner using a mask.

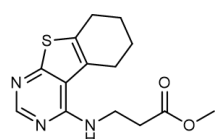
10-precondition set test

Supplementary Table 1 10-precondition set (Figure 4 of main text)

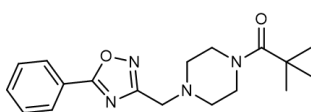
Set #	#1	#2	#3	#4	#5	#6	#7	#8	#9	#10
logP	2.424	2.240	3.166	1.685	1.395	3.180	2.808	2.684	3.301	1.121
tPSA	63.32	54.48	68.43	86.48	64.43	55.41	81.49	50.20	65.10	81.80
QED	0.870	0.842	0.581	0.847	0.756	0.857	0.852	0.844	0.544	0.901

Supplementary Table 1 shows the details of precondition sets used in the test shown in Figure 4 of the main text. The sets were determined by dividing 1,000 intervals between the minimum and maximum values for each property, drawing a three-dimensional histogram, and random sampling from the probability that training samples exist in each cell.

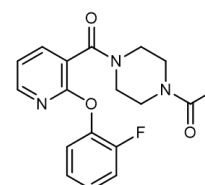
Supplementary Figures 1-10 are the first 9-molecules generated for each precondition set.



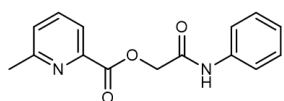
COC(=O)CCNc1ncnc2sc3c(c12)CCCC3
2.545, 64.11, 0.877, 31



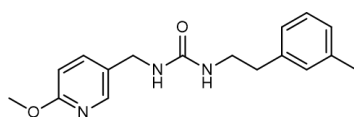
CC(C)(C)C(=O)N1CCN(Cc2noc(-c3ccccc3)n2)CC1
2.427, 62.47, 0.866, 42



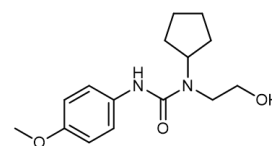
CC(=O)N1CCN(C(=O)c2cccnc2Oc2ccccc2F)CC1
2.317 62.74 0.858, 39



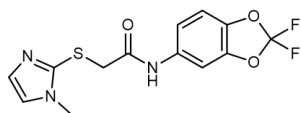
Cc1cccc(C(=O)OCC(=O)Nc2ccccc2)n1
2.185, 68.29, 0.865, 32



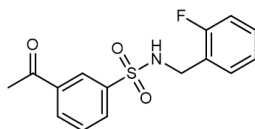
COc1ccc(CNC(=O)NCCc2cccc(C)c2)cn1
2.441, 63.25, 0.861, 33



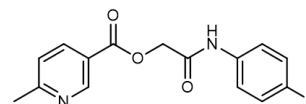
COc1ccc(NC(=O)N(CCO)C2CCCC2)cc1
2.464, 61.80, 0.869, 31



Cn1ccnc1SCC(=O)Nc1ccc2c(c1)OC(F)(F)O2
2.472, 65.38, 0.874, 37



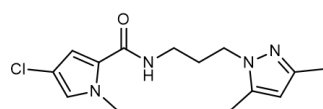
CC(=O)c1cccc(S(=O)(=O)NCc2cccc(c2F)c1
2.507, 63.24 0.863, 36



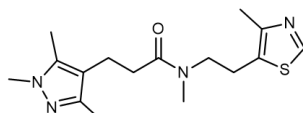
Cc1ccc(C(=O)OCC(=O)Nc2ccc(F)cc2)cn1
2.325, 68.29, 0.877, 35

Supplementary Figure 2. First 9-generated molecules at the given precondition set #1. The string below the molecule image is the SMILES string. The four numbers below that

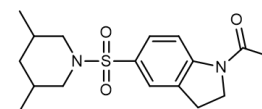
are actual logP, tPSA, QED, and the number of tokens, respectively.



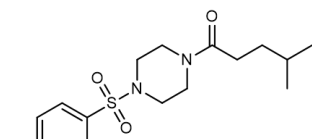
Cc1cc(C)n(CCCNC(=O)c2cc(C)cn2C)n1
2.312, 51.85, 0.861, 33



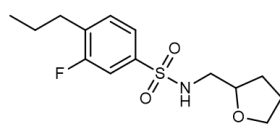
Cc1nn(C)c(C)c1CCC(=O)N(C)CCc1scnc1C
2.436, 51.02, 0.821, 35



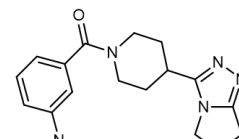
CC(=O)N1CCc2cc(S(=O)(=O)N3CC(C)CC(C)C3)ccc21
2.262, 57.69, 0.832, 44



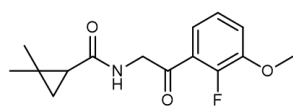
Cc1ccc(S(=O)(=O)N2CCN(C(=O)CCC(C)C)CC2)cc1
2.264, 57.69, 0.827, 42



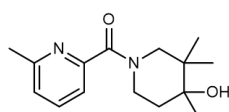
CCCc1ccc(S(=O)(=O)NCC2CCCO2)cc1F
2.236, 55.4, 0.876, 32



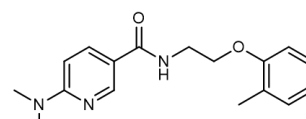
CN(C)c1cccc(C(=O)N2CCC(c3nnc4n3CCC4)CC2)c1
2.310, 54.26, 0.861, 42



COc1cccc(C(=O)CNC(=O)C2CC2(C)C)c1F
2.179, 55.4, 0.840, 34

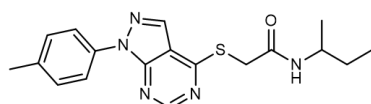


Cc1cccc(C(=O)N2CCC(C)(O)C(C)C)C2)n1
2.013, 53.43, 0.842, 36

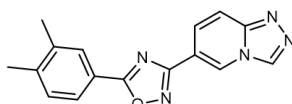


Cc1cccc1OCCN(C(=O)c1ccc(N(C)C)nc1)
2.265, 54.46, 0.831, 33

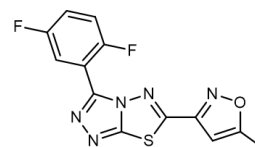
Supplementary Figure 3. First 9-generated molecules at the given precondition set #2.



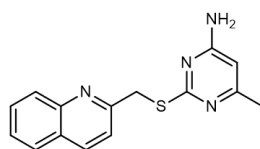
CCC(C)NC(=O)CSc1ncnc2c1cnn2-c1ccc(C)cc1
3.131, 72.70, 0.543, 39



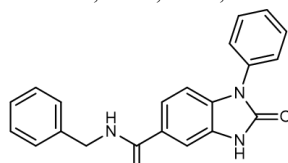
Cc1ccc(-c2nc(-c3ccc4nncn4c3)no2)cc1C
3.063, 69.11, 0.567, 36



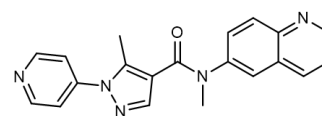
Cc1cc(-c2nn3c(-c4cc(F)ccc4F)nnc3s2)no1
3.094, 69.11, 0.568, 38



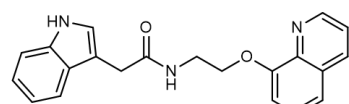
Cc1cc(N)nc(SCc2ccc3cccc3n2)n1
3.208, 64.69, 0.590, 30



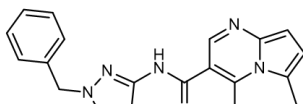
O=C(NCc1cccc1)c1ccc2c(c1)[nH]c(=O)n2-c1cccc1
3.249, 66.89, 0.597, 43



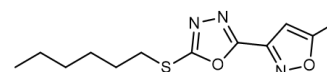
Cc1c(C(=O)N(C)c2ccc3ncccc3c2)cn1-c1ccncc1
3.401, 63.91, 0.572, 42



O=C(Cc1c[nH]c2cccc12)NCCOc1ccc2ccncc12
3.454, 67.01, 0.526, 37

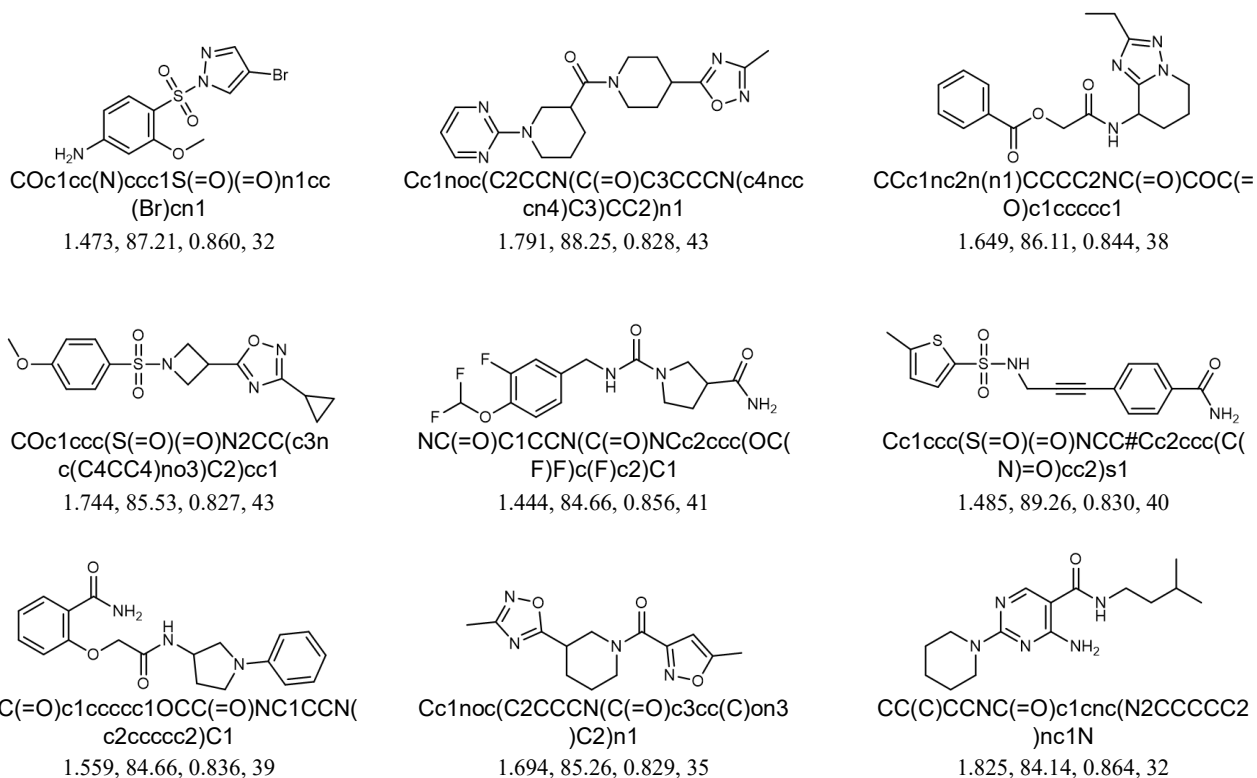


Cc1ccc2ncc(C(=O)Nc3ccn(Cc4cccc4)n3)c(C)n21
3.448, 64.22, 0.616, 43

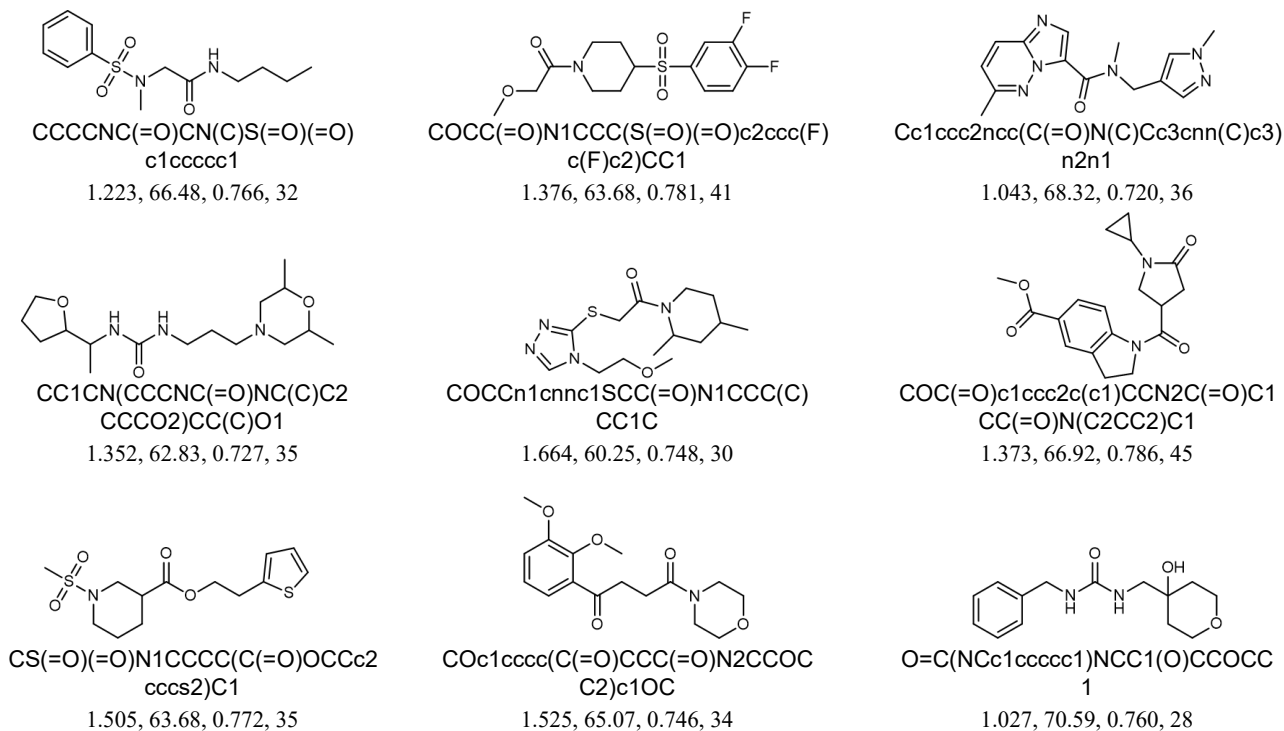


CCCCCSc1nnc(-c2cc(C)on2)o1
3.705, 64.95, 0.563, 27

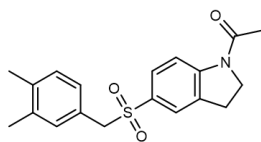
Supplementary Figure 4. First 9-generated molecules at the given precondition set 3.



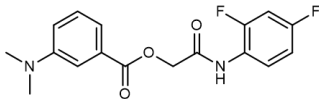
Supplementary Figure 5. First 9-generated molecules at the given precondition set 4.



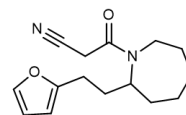
Supplementary Figure 6. First 9-generated molecules at the given precondition set 5.



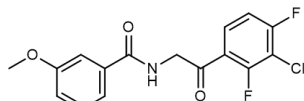
CC(=O)N1CCc2cc(S(=O)(=O)C
c3ccc(C)c(C)c3)ccc21
3.186, 54.45, 0.860, 45



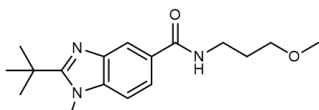
CN(C)c1cccc(C(=O)OCC(=O)Nc2ccc(F)cc2F)c1
2.826, 58.64, 0.854, 40



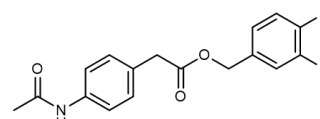
N#CCC(=O)N1CCCCC1CCc1ccc1
2.897, 57.24, 0.836, 27



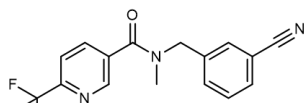
COc1cccc(C(=O)NCC(=O)c2c
cc(F)c(Cl)c2F)c1
3.240, 55.4, 0.672, 39



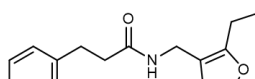
COCCCN(C(=O)c1ccc2c(c1)nc(C(C)C)C)n2C
2.637, 56.15, 0.864, 37



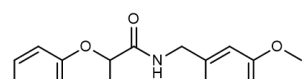
CC(=O)Nc1ccc(CC(=O)OCc2ccc(F)c(F)c2)cc1
3.209, 55.4, 0.861, 39



CN(Cc1cccc(C#N)c1)C(=O)c1ccc(C(F)(F)F)nc1
3.244, 56.99, 0.872, 41

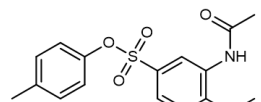


CCc1noc(CC)c1CNC(=O)CCc1cccc1F
3.188, 55.13, 0.854, 31

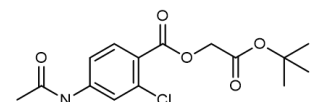


COc1ccc(CNC(=O)C(C)Oc2ccccc2C)cc1OC
3.096, 56.79, 0.848, 35

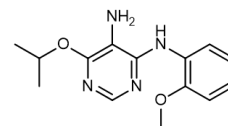
Supplementary Figure 7. First 9-generated molecules at the given precondition set 6.



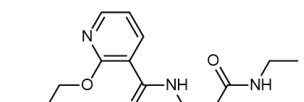
COc1ccc(S(=O)(=O)Oc2ccc(C)cc2)cc1NC(=O)
2.730, 81.70, 0.850, 40



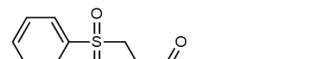
CC(=O)Nc1ccc(C(=O)OCC(=O)OC(C)C)c(Cl)c1
2.797, 81.70, 0.860, 41



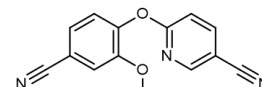
CCOc1ccccc1Nc1ncnc(OC(C)C)c1N
2.988, 82.29, 0.850, 29



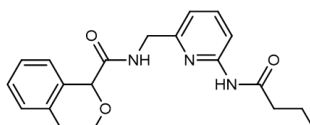
CCNC(=O)c1cccc1NC(=O)c1ccncc1OCC(F)F
2.728, 80.32, 0.805, 37



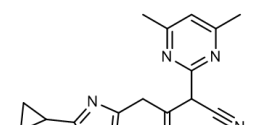
CC(=O)c1ccc(NC(=O)CCS(=O)(=O)c2ccccc2)cc1
2.692, 80.31, 0.825, 41



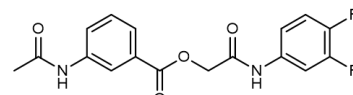
COc1cc(C#N)ccc1Oc1ccc(C#N)cn1
2.626, 78.93, 0.837, 29



CCCC(=O)Nc1cccc(CNC(=O)C2OCc3ccccc32)n1
2.750, 80.32, 0.837, 40

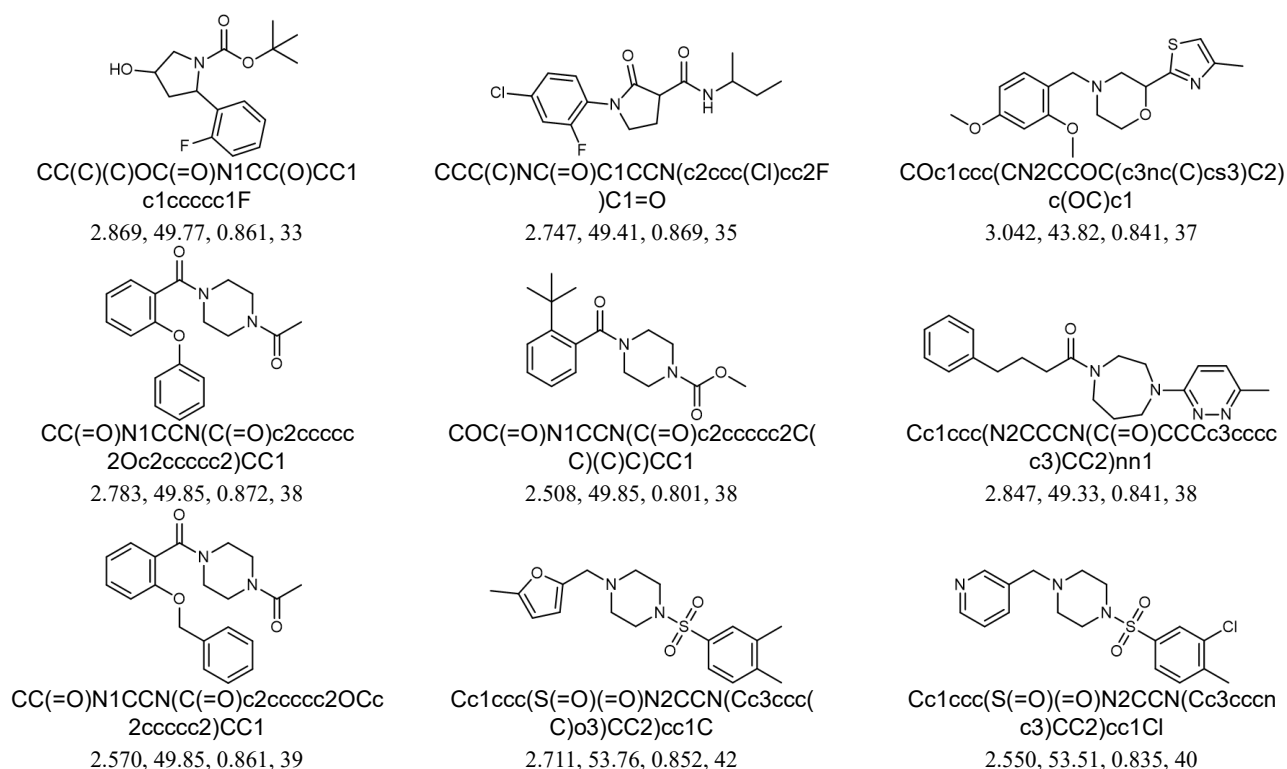


Cc1cc(C)nc(C(C#N)C(=O)Cc2csc(C3CC3)n2)n1
2.846, 79.53, 0.848, 40

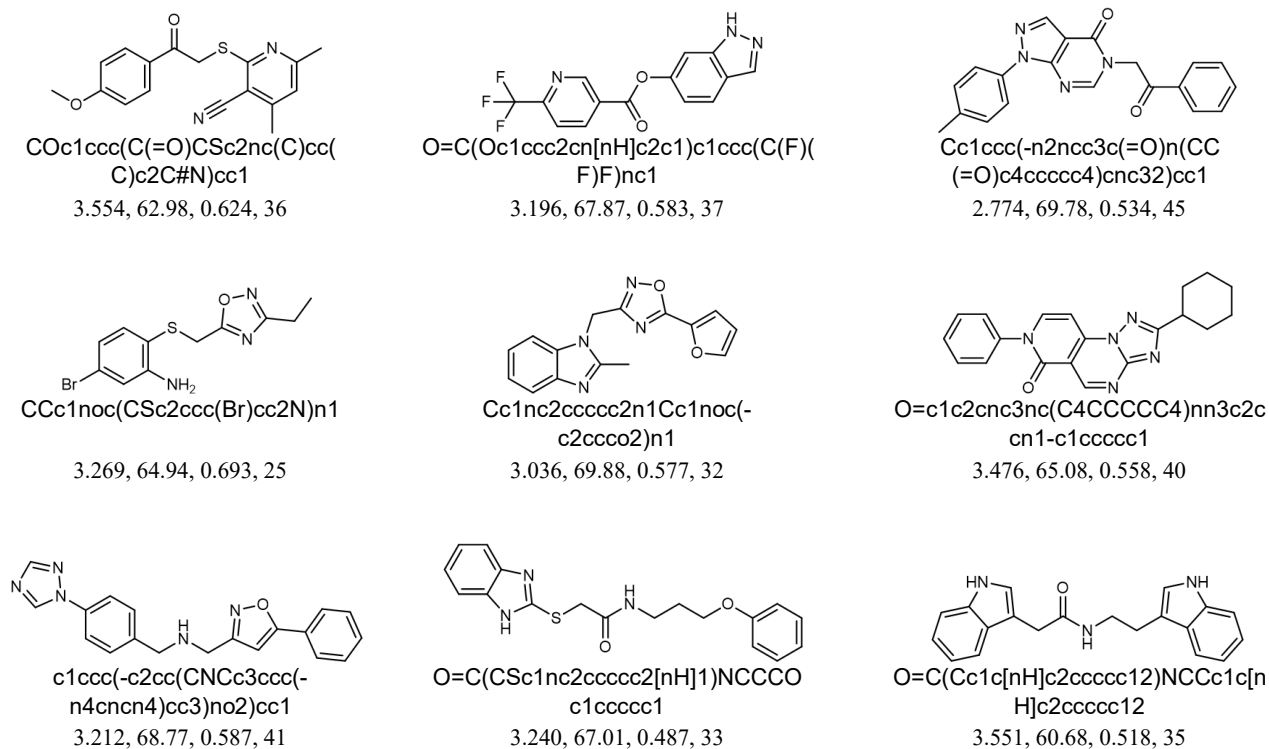


CC(=O)Nc1cccc(C(=O)OCC(=O)Nc2ccc(F)c(F)c2)c1
2.719, 84.5, 0.814, 44

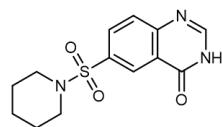
Supplementary Figure 8. First 9-generated molecules at the given precondition set 7.



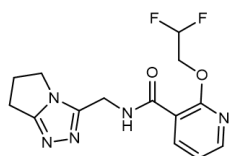
Supplementary Figure 9. First 9-generated molecules at the given precondition set 8.



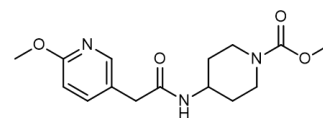
Supplementary Figure 10. First 9-generated molecules at the given precondition set 9.



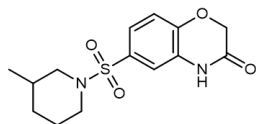
O=c1[nH]cnc2ccc(S(=O)(=O)N3CCCC3)cc12
1.098, 83.13, 0.898, 35



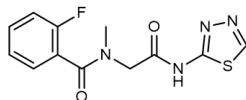
O=C(NC1nnc2n1CCC2)c1cccnc1OC
C(F)F
1.193, 81.93, 0.863, 34



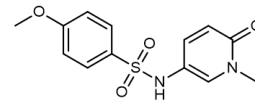
COC(=O)N1CCC(NC(=O)Cc2ccc(OC)nc2)CC1
0.980, 80.76, 0.897, 36



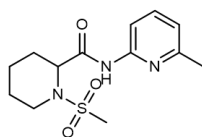
CC1CN(S(=O)(=O)c2ccc3c(c2)NC(=O)CO3)CCC1
1.438, 75.71, 0.897, 40



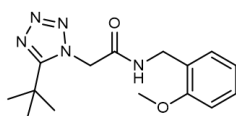
CN(CC(=O)Nc1nncs1)C(=O)c1ccccc1F
1.388, 75.19, 0.924, 32



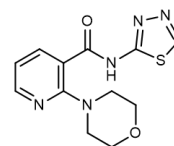
COc1ccc(S(=O)(=O)Nc2ccc(=O)n(C)c2)cc1
1.195, 77.4, 0.919, 37



Cc1cccc(NC(=O)C2CCCN2S(C)(=O)=O)n1
1.143, 79.37, 0.907, 35



COc1ccccc1CNC(=O)Cn1nnc1C(C)(C)C
1.296, 81.93, 0.900, 33



O=C(Nc1nncs1)c1cccnc1N1CCOCC1
1.022, 80.24, 0.909, 29

Supplementary Figure 11. First 9-generated molecules at the given precondition set 9.

References

1. Sohn, K., Lee, H. & Yan, X. Learning structured output representation using deep conditional generative models. *Advances in neural information processing systems* **28**, 3483-3491 (2015).
2. Xiong, R. et al. On layer normalization in the transformer architecture. *In proceedings of International Conference on Machine Learning* 10524-10533 (2020).